Efficient Filter Bank Multicarrier Realizations for 5G

Leonardo G. Baltar, Israa Slim, Josef A. Nossek
Institute for Circuit Theory and Signal Processing
Technische Universität München, 80290 Munich, Germany
Email: leo.baltar@tum.de

***Abstract*—In this contribution we compare different realizations of the polyphase networks employed in Offset QAM based Filter Bank Multicarrier (OQAM-FBMC). Our objective is to evaluate the structures' computational cost and robustness for very low complexity implementations of the prototype filter coefficients. We compare a direct form, a classical lattice realization, where in both the Canonical Signed Digit (CSD) representation of the coefficients is applied, and a Coordinate Rotation by Digital Computer (CORDIC)-based lattice structure. We evaluate the cost after coefficient quantization in terms of number of additions and shifts. By considering the multicarrier application, we show the effects of coefficient quantization on the subcarrier filters spectrum and on the multicarrier transmit signal Power Spectral Density (PSD).**

I. Introduction

FBMC systems are currently strong candidates for the fifth generation (5G) of mobile communications standards. Among them, OQAM-FBMC appears as a very competitive approach. Because of the wide range of applications envisioned for 5G, including low cost mobile stations, e.g. sensors, an efficient implementation of the waveform generation is necessary.

Multiplication by the prototype filter coefficients are the very costly operations in FBMC modulation. After the design of the prototype filter, the coefficients obtained are represented with the accuracy of the computer employed, usually in high resolution floating point representation. However, in efficient practical implementations they will be realized with low resolution fixed-point arithmetic in Digital Signal Processors (DSPs) or VLSI ASIC chips. In this case, the coefficients have to be quantized, usually using rounding, and the time and frequency responses will deviate from the originals. If the subcarrier frequency response or the out-of-band radiation have to meet some prescribed specification, the quantized prototype may even fail to do that. Moreover, the sensitivity to coefficient quantization depends on the filter structure employed and this is the main motivation of this study. Therefore, we perform a comparison of different realization structures.

By using a fixed-point binary representation of the coefficients, e.g. two's complement, the multiplication can be substituted by shifts and additions. However, using an ordinary binary representations will require a large number of shifts and additions. An alternative representation is the CSD representation [1], [2] that also includes subtractions. In addition to that, CSD minimizes the number of non-zero digits by avoiding them to be consecutive and thus reducing the number of partial product additions/subtractions. The shift operations can be implemented by only connecting the wires to the corresponding bit positions or by using shift registers. The hardware complexity can then be evaluated in terms of the total number of additions/subtractions and shift operations. It is worth noting that the output signal word-length will determine the maximum size of the shift registers. We also assume here that input and output word-lengths are identical.

The critically sampled Modulated Filter Banks (MFBs) have very efficient structures that allow the implementation of pairs of polyphase components using lattice structures, that preserve perfect reconstruction (PR)[3] even after quantization. Moreover, the lattice structures can be implemented using CORDIC [4], [5] in order to improve the quality of the quantized coefficients with reduced complexity.

II. Efficient Modulated Filter Bank Structure

We consider here uniform exponential MFBs. In uniform FBs, all subchannels have the same sampling rate $1/T$, all analysis $H_k(z)$ and synthesis filters $F_k(z)$ in the subchannels have the same bandwidth and are derived from a single prototype filter denoted as $H_{\mathrm{P}}(z)$. In those FBs, both $H_k(z)$ and $F_k(z)$ are obtained by exponentially modulating $H_{\mathrm{P}}(z)$ as

$$H_k(z) = F_k(z) = H_P(zW_M^k)d^k, \quad k = 0, 1, \ldots, M-1, \quad (1)$$

where M is the number of subchannels and

$$H_{\mathrm{P}}(z) = H_0(z) = \sum_{p=0}^{P-1} h_p z^{-p},$$

$$H_k(z) = \sum_{p=0}^{P-1} h_{k,p} z^{-p}, \quad h_{k,p} = h_p W_M^{-k\left(p-\frac{P-1}{2}\right)}, \quad (2)$$

with $W_M = e^{-j\frac{2\pi}{M}}$ and $d = e^{j\frac{2\pi}{M}\frac{P-1}{2}}$. We also assume here without loss of generality that the length of the prototype $P = KM$, where K is a time overlap factor and determines not only the complexity of the filter bank, but also its memory.

An efficient structure of the Synthesis Filter Bank (SFB) is shown in Fig. 1, where $G_m(z^M), m = 0, ..., M-1$, is the m-th type-1 polyphase component of $H_{\mathrm{P}}(z)$ according to the relation

$$H_P(z) = \sum_{m=0}^{M-1} G_m(z^M) z^{-m}. \quad (3)$$

Since we have assumed that the prototype has a length of KM, each polyphase component will have K coefficients.

The block $\mathcal{O}_k$ performs a $\frac{T}{2}$ OQAM staggering of the real and imaginary parts of the low-rate signals $x_k[m]$. Fig. 2 depicts the internal structure of $\mathcal{O}_k$ for even k. For odd k the $\mathrm{Re}\{\bullet\}$ and $j\mathrm{Im}\{\bullet\}$ blocks are exchanged.

We assume here that the prototype filter $H_{\mathrm{P}}(z)$ was designed such that PR [2], [3], [6] is fulfilled. In that case,

978-1-4799-8391-9/15/$31.00 ©2015 IEEE

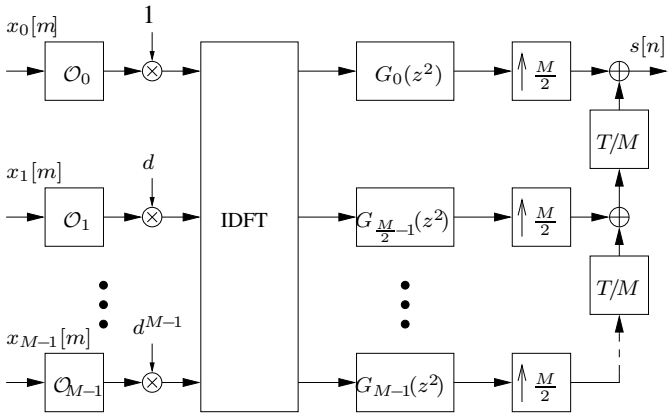

Figure 1. Polyphase network based efficient structure of SFB

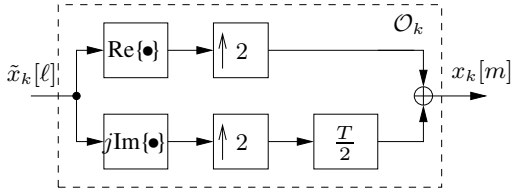

Figure 2. OQAM-Staggering Operation for even k

and in ideal channel conditions, the subcarriers are completely orthogonal. Furthermore, the prototype has to have a symmetrical impulse response. In general, the methods to design the prototype filter $H_P(z)$ to guarantee PR set constraints on the polyphase filters [7]. For the case that the prototype filter has a length of $P = 2M$ ($K = 2$), there exists a closed form expression of the filter's coefficients h_p, the so called Extended Lapped Transform (ELT) [8]:

$$h_p = \frac{-1}{4} + \frac{1}{2}\cos\left(\frac{\pi}{2M}(2p+2M)\right), \quad p = 0, ..., 2M-1. \quad (4)$$

For the cases where $K > 2$ there is no closed form solution and the prototype has to be obtained by numerical optimization methods [2], [9], [10].

It is worth noting that, although the PR prototype has a symmetrical impulse response, one multiplier per coefficient has to be realized in the polyphase network.

III. Polyphase Components Realized with Lattice

Regarding Fig. 1 again, it is possible to show that $M/2$ pairs of polyphase components are power complementary [3], [6]. The terms $G_k(z^2)$ and $G_{k+\frac{M}{2}}(z^2)$ possess this property thus can be grouped as shown in Fig. 3, where the permutation matrix $\mathbf{P}$ is necessary to reorganize the IDFT outputs.

The polyphase components pairs can be jointly implemented using a non-recursive lattice structure [3], [5]. The lattice structure of each pair of the polyphase components is shown in Fig. 4, where the rotations $\mathbf{R}_{k,i}, i = 0, ..., K-2$ are mathematically defined by

$$\mathbf{R}_{k,i} = \begin{bmatrix} \cos\Theta_{k,i} & \sin\Theta_{k,i} \\ -\sin\Theta_{k,i} & \cos\Theta_{k,i} \end{bmatrix},$$

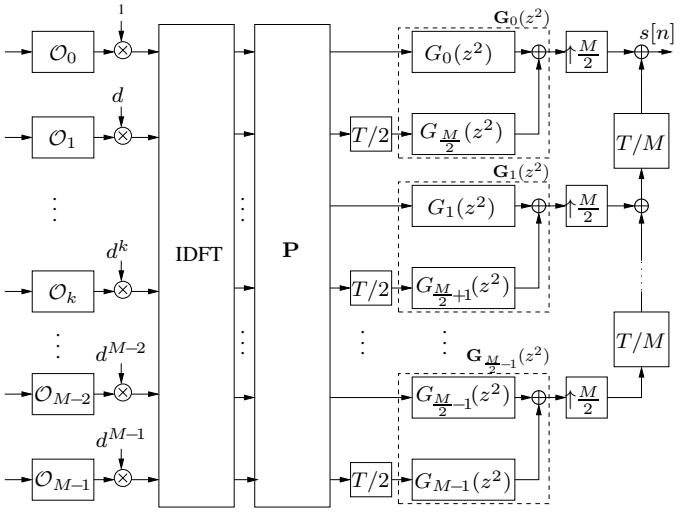

Figure 3. Efficient SFB structure with reordered polyphase components

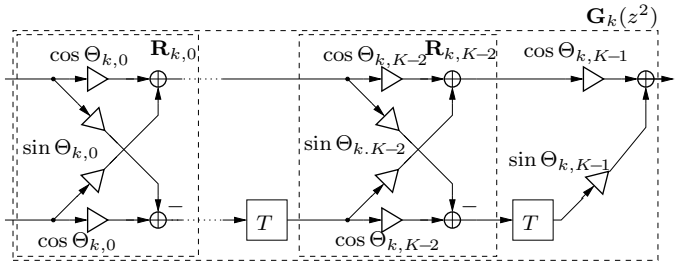

Figure 4. Lattice realization of polyphase matrix

where we have dropped the index k to simplify the notation. The Θ_is are calculated from the polyphase components transfer function by a successive polynomial degree reduction [3].

We can also quantize the 4 coefficients of the lattice rotors using the CSD representation. And again the multiplication can be implemented by shifts and additions. Since the coefficients are sines and cosines, the dynamic range is already normalized. The main advantage of the lattice structure is that PR is preserved even after quantization.

The problem is that the structure in Fig. 4 has a higher complexity than the direct form. For this reason, we can modify the rotors to have only two multipliers and, additionally, two multipliers for each polyphase component, as shown in Fig. 5, where $\kappa_k = \prod_{i=0}^{K-1} \cos\Theta_{k,i}$. Although now the complexity is considerably reduced, the coefficients are tangent functions and their dynamic range, depending on the resulting angles, are theoretically unlimited. It becomes hard to find an optimum quantizer step-size and the frequency behavior of the filters depends a lot on this choice. As an alternative, we can use CORDIC-based rotors [5], [11].

IV. CORDIC-based Lattice Rotation

To avoid the direct computation of the trigonometric function $\tan\Theta_{k,i}$ the rotation by the angle $\Theta_{k,i}$ is successively approximated by a sequence of elementary (micro-) rotations by the angles $\sigma_{k,i,w}\alpha_w$, $\sigma_{k,i,w} = \{-1, 0, +1\}$, $w = 0, 1, \ldots, W-1$. These are chosen in such a way that $\tan\alpha_w = 2^{-w}$, which for binary data only requires a simple

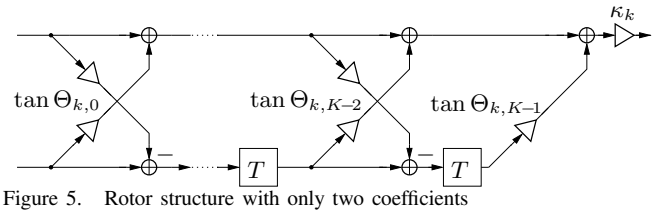

Figure 5. Rotor structure with only two coefficients

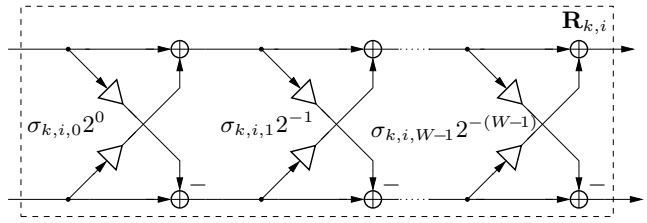

Figure 6. CORDIC based realization of one lattice rotor

shift by w bits. Thus, we have

$$\Theta_{k,i} \approx \sum_{w=0}^{W-1} \sigma_{k,i,w}\alpha_w = \sum_{w=0}^{W-1} \sigma_{k,i,w} \arctan(2^{-w}),$$
$$0 < |\Theta_{k,i}| < \frac{\pi}{4}, \quad \sigma_{k,i,w} = \{-1, 0, +1\}, \qquad (5)$$

where the sign factor $\sigma_{k,i,w}$ is chosen according to the different CORDIC algorithms as Elementary-Angle-Set Angle Recoding (EAS-AR) [4], [12] and the extended CORDIC structures that promise higher precision for the same complexity like, for example, Extended EAS-AR [4]. The total number of approximation steps W depends on the required accuracy. If the word-length of the input and the output data is b bits, the least significant bit has weight 2^{-b}, which should be equal to the smallest angle $\arctan 2^{-W} \approx 2^{-W}$. So, we stop at $W = b$.

Each rotor can be now implemented as in the structure in Fig. 6, where the multipliers are now only shifts and if $\sigma_{k,i,w} = 0$ the micro-rotation will become trivial and neither shift nor additions/subtractions need to be implemented.

V. Numerical Evaluation

To evaluate the effect of coefficient quantization in an FBMC system we consider here a total of $M = 128$ subcarriers. Two prototypes with different lengths will be considered: for $K = 2$ we took the ELT from (4) and for $K = 4$ we took a PR optimized prototype that minimizes the energy in the stop-band in a Least Squares (LS) sense using the method presented in [10], [13].

We consider three structures: direct form, classical lattice and CORDIC-based lattice. For the first two, the coefficients are directly quantized using CSD representation. Furthermore, for the direct form, the dynamic range of the quantizer is adjusted to minimize the effects of saturation. For the classical lattice no such adjustment is needed, because the coefficients are limited to one. For the CORDIC-based lattice, we have employed the EAS-AR algorithm to calculate the micro-rotations. Finally, for the κ_ks we have employed a modified Booth's (multiplier) recoding representation as in [12].

To evaluate the different structures after coefficient quantization, we have considered first the total number of additions and subtractions for the realization of the polyphase network

Word-length	Direct Form		Classical lattice		Lattice-CORDIC	
	ELT	LS-PR	ELT	LS-PR	ELT	LS-PR
8	602	892	1192	2516	525	1177
10	778	1216	1468	3104	683	1460
12	952	1576	1712	3716	843	1796
14	1120	1926	1964	4320	977	2124

Table I. Number of additions and subtractions for the ELT ($K = 2$) and LS-optimized PR prototype ($K = 4$)

Word-length	Direct Form		Classical lattice		Lattice-CORDIC	
	ELT	LS-PR	ELT	LS-PR	ELT	LS-PR
8	730	1020	1064	2132	260	944
10	906	1344	1340	2720	353	1177
12	1080	1704	1584	3332	434	1442
14	1248	2054	1836	3936	519	1703

Table II. Number of shifters for the ELT ($K = 2$) and LS-optimized PR prototype ($K = 4$)

in the SFB. We assume that the complexity of the DFT will be the same for all structures and we therefore do not include it in the comparison.

In Table I the total number of additions are listed for different word-lengths and for both prototypes. For the ELT, one can see that the classical lattice needs a much higher number of additions and subtractions compared to the other two structures, with the Lattice-CORDIC exhibiting a reduction of about 13%. Of course both lattice structures preserve the orthogonality between the subcarriers as opposed to the direct form that does not. In the case of the LS-optimized prototype, the complexity of the classical lattice structure increases by more than 2 times compared to the direct form, but for the lattice-CORDIC it increases by 10 to 30%.

In Table II the total number of shifters are given for different word-lengths and for two prototypes. For the ELT we can see that the lattice-CORDIC has a much lower number and the classical lattice has more than 50% increase compared to the direct form. In the case of the longer prototype the lattice-CORDIC has a reduction from 8 to 18% compared to the direct form.

As a second figure of merit to illustrate the effects of coefficient quantization we have examined the frequency response of the subcarrier filters, i.e. the prototype frequency response, for all the three structures and for unquantized direct form. In Fig. 7 we have depicted the frequency response for $W = 10$ for ELT. We can see no significant deviation can be observed compared to the direct form for all structures. Again, one should note that only lattice structures preserve the orthogonality.

In Fig. 8 we have plotted the frequency responses for the LS-optimized PR prototype for $W = 12$. Only the lattice-CORDIC shows a strong deviation in the stop-band but for higher Ws no deviations were observed.

In order to observe the quantization effects in the out-of-band radiation of the transmitted multicarrier signals, we have calculated the estimated power spectrum densities (PSD). A total of 1000 QPSK symbols per subcarrier were sent through the SFB and its outputs were used for the PSDs estimation. Only $M_u = 76$ of the $M = 128$ subcarriers were occupied. We have then employed the Welch's method [14] with an FFT size of 2048, an overlapping of 50% and a Kaiser window with $\beta = 5$ to plot the PSDs.

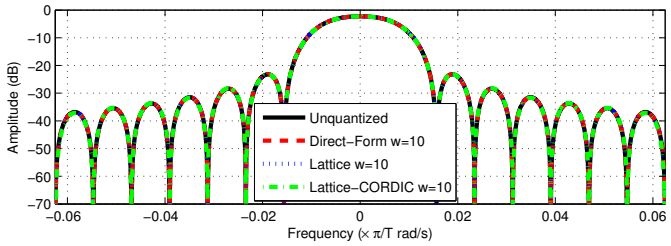

Figure 7. Subcarrier filter frequency response for the ELT ($K = 2$) with word-length $W = 10$

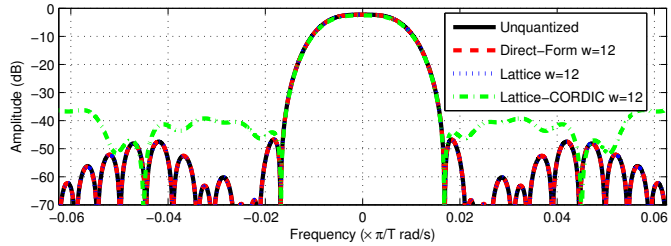

Figure 8. Subcarrier filter frequency response for the LS-optimized PR prototype with $K = 4$ and word-length $W = 12$

In Fig. 9 the PSDs for the ELT with $W = 8$ and $W = 10$ are depicted. In the first case all the structures exhibit no deviation except the Lattice-CORDIC with 17 dB higher out-of-band radiation compared to the unquantized structure. But for $W = 10$ even the Lattice-CORDIC shows no deviation.

Fig. 10 shows the PSDs for the LS-optimized PR prototype with $W = 12$ and $W = 14$. The deviations for $W = 12$ is almost 30 dB for the lattice-CORDIC compared to the unquantized case. For $W = 14$ no deviation is observed.

VI. Conclusions

For shorter prototypes, e.g. ELT, the Lattice-CORDIC structure presents lower complexity in terms of number of additions and shifters compared to the CSD quantized direct form and even lower compared to classic Lattice. For longer prototypes, a small increase in the complexity in terms of number of additions is observed, but a much lower number of shifters are required. However, for shorter word-lengths it is necessary to consider more advanced CORDIC structures that provide better rotation angle approximation without increased complexity in order to obtain good spectral behavior.

A classical Lattice structure has the advantage to preserve PR, i.e. orthogonality between subcarriers, even when the coefficients are quantized. It is expected that a Lattice-CORDIC structure with a better angle approximation should have more robustness to the coefficient quantization, specially for shorter word-lengths, when compared to direct form.

To summarize, since for 5G applications a good spectral containment of the multicarrier system based on filter banks is expected, one should be careful in the choice of the efficient implementation when considering finite word-length effects.

Acknowledgment

This work was partially supported by the EU project EMPhAtiC (ICT-318362).

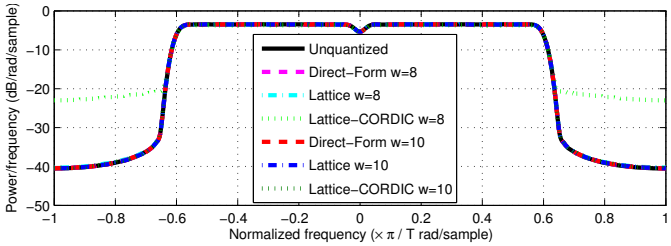

Figure 9. Welch's PSD of the transmitted signal for the ELT ($K = 2$) and word-lengths $W = 8$ and $W = 10$

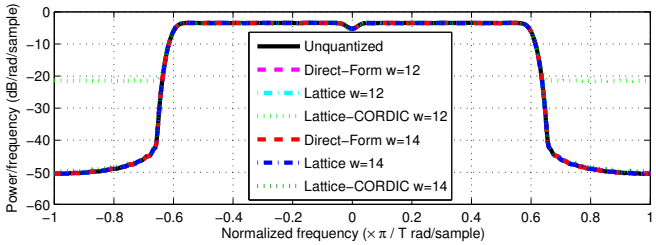

Figure 10. Welch's PSD of the transmitted signal for the LS-optimized PR prototype with $K = 4$ and word-lengths $W = 12$ and $W = 14$

References

[1] K. Hwang, *Computer arithmetic: principles, architecture, and design*, ser. Computer Arithmetic: Principles, Architecture, and Design. Wiley, 1979, no. v. 1.

[2] P. Diniz, E. da Silva, and S. Netto, *Digital Signal Processing: System Analysis and Design*, ser. E-Libro. Cambridge University Press, 2010.

[3] P. P. Vaidyanathan, *Multirate Systems and Filter Banks*. Englewood Cliffs, NJ: Prentice-Hall, 1993.

[4] P. K. Meher, J. Valls, T.-B. Juang, K. Sridharan, and K. Maharatna, "50 years of CORDIC: Algorithms, architectures, and applications," *IEEE Trans. Circuits Syst. I*, vol. 56, no. 9, pp. 1893–1907, 2009.

[5] T. Karp, A. Mertins, and T. Q. Nguyen, "Efficiently VLSI-realizable prototype filters for modulated filter banks," in *Acoustics, Speech, and Signal Proces., ICASSP-97, IEEE Int. Conf. on*, vol. 3, 1997, pp. 2445–2448.

[6] N. J. Fliege, *Multirate Digital Signal Processing*. Chichester,U.K.: Wiley, 1994.

[7] T. Karp and N. Fliege, "Modified DFT filter banks with perfect reconstruction," *IEEE Trans. Circuits Syst. II*, vol. 46, no. 11, pp. 1404–1414, Nov. 1999.

[8] H. S. Malvar, *Signal Processing with Lapped Transforms*. Norwood, MA: Artech Hause, 1992.

[9] A. Viholainen, *Modulated Filter Bank Design for Communications Signal Processing*. Tampere University of Technology, 2004.

[10] T. Saramaki, "A generalized class of cosine-modulated filter banks," in *Proc. TICSP Workshop on Transforms and Filter Banks*, Tampere, Finland, Jun. 1998, pp. 336–365.

[11] S. Simon, P. Rieder, C. Schimpfle, and J. A. Nossek, "CORDIC-based architectures for the efficient implementation of discrete wavelet transforms," in *Circuits and Syst., ISCAS '96, IEEE Int. Symp. on*, vol. 4, 1996, pp. 77–80.

[12] Y. H. Hu and S. Naganathan, "Angle recoding method for efficient implementation of the CORDIC algorithm," in *Circuits and Syst., ISCAS 1989., IEEE Int. Symp. on*, 1989, pp. 175–178.

[13] M. B. Furtado, P. S. R. Diniz, and S. L. Netto, "Numerically efficient optimal design of cosine-modulated filter banks and transmultiplexers with peak-constrained least-squares behavior," *IEEE Trans. on Circuits and Syst. I*, vol. 52, no. 3, pp. 597–608, March 2005.

[14] A. Oppenheim, R. Schafer, and J. Buck, *Discrete-Time Signal Processing*, 2nd ed. Upper Saddle River, NJ, EUA: Prentice-Hall, 1997.